

# Progress of SONIC simulations for divertor detachment in EU DEMO and He exhaust in JA DEMO (Report from Project SSDEMO)

Nobuyuki Asakura<sup>1</sup>, K. Hoshino<sup>2</sup>, Y. Homma<sup>3</sup>, F. Subba<sup>4</sup>, S. Wiesen<sup>5</sup>

<sup>1</sup>National Institutes for Quantum and Radiological Science and Technology (QST), Naka,  
<sup>2</sup>Keio University, Yokohama, <sup>3</sup>QST, Rokkasho,  
<sup>4</sup>Politecnico di Torino, Torino, <sup>5</sup>Forschungszentrum Juelich GmbH, Juelich

13 May 2022

IFERC-CSC Workshop on JFRS-1 projects for FY2021, On-line meeting

## 1. SONIC simulation for EU-DEMO divertor

⇒ First step of Benchmark between SONIC and SOLPS-ITER

## 2. He exhaust simulation by SONIC for JA-DEMO divertor

⇒ Particle exhaust and optimization of the DEMO divertor design

### Acknowledgments:

JFRS-1 was used for key exhaust parameter survey such as  $n_e^{\text{mid}}$  and diffusion coefficients and model development for the JA DEMO divertor operation. Recent publications are as following,

- [1] Asakura, N.; Hoshino, K.; Homma, Y.; Sakamoto, Y.; Joint Special Design Team for Fusion DEMO; Simulation studies of divertor detachment and critical power exhaust parameters for Japanese DEMO design. Nucl. Mater. Energy 2021, 26, 100864.
- [2] Asakura, N.; Hoshino, K.; Kakudate, S.; Subba, F.; Vorpahl, C.; Homma, Y.; Utoh, H.; Someya, Y.; Sakamoto, Y.; Hiwatari, R.; et al. Power Exhaust Concepts and Divertor Designs for Japanese and European DEMO Fusion Reactors. Nucl. Fusion 2021, 61, 126057 (15pp).
- [3] Homma, Y.; Assessment of the impact of the kinetic effect of ion parallel heat conduction on DEMO-relevant SOL plasma using integrated SOL-divertor code SONIC, Plasma Phys. Control. Fusion 64 (2022) 045020 (14pp).
- [4] Asakura, N.; Hoshino, K.; Homma, Y.; Sakamoto, Y.; Joint Special Design Team for Fusion DEMO; Development and Application of SONIC Divertor Simulation Code to Power Exhaust Design of Japanese DEMO Divertor, accepted in PROCESSES (2022).



# Development of SONIC V4 and recent progresses

-3-

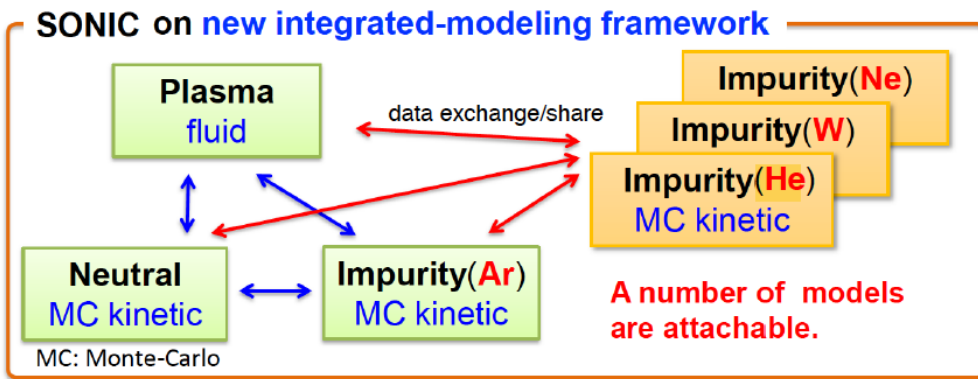
• Modeling framework using MPMD (Multiple-Program Multiple-Data) approach and MPI (Message Passing Interface) data exchange scheme has been developed for

- (1) Each code can be independently developed, added and replaced.
- (2) Improved numerical efficiency: e.g. number of CPUs used for each code can be arbitrarily adjusted to optimize performance.

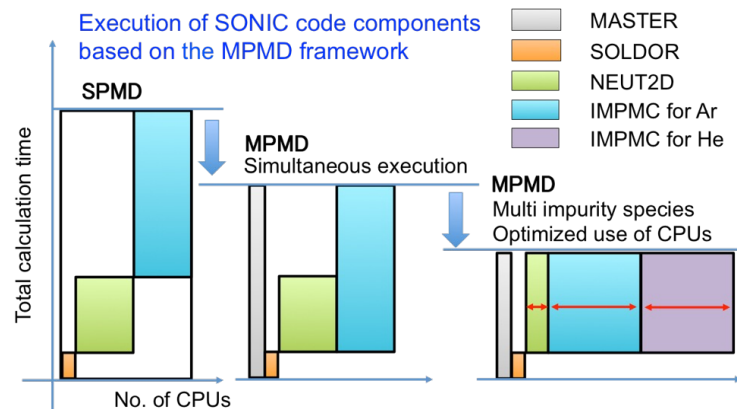
⇒ Power and particle exhaust of DEMO divertor, consistent with Ar and He transports, has been recently simulated.

## (1) Restructured SONIC code with MPMD framework

integrated divertor code, SONIC



## (2) Improved numerical efficiency for multi-impurity calculation



Recent progresses of modelling to evaluate influences under the DEMO condition:

- Kinetic models of thermal force on impurity transport and flux limiter for ion conduction for low collisionality SOL in DEMO were developed [5, 3].
- Elastic collision model of D-D, D-D<sub>2</sub>, D<sub>2</sub>-D<sub>2</sub>, D-He was incorporated, and improvement is in progress [6].
- Self-consistent photon transport simulation was performed for SlimCS [7] and JA DEMO.

[5] Y. Homma, et al, Nucl. Fus.60 (2020) 046031, [6] K. Hoshino, et al., PET-18 (2021) [7] K. Hoshino, et al., Contrib. Plasma Phys., 56 (2016) 657.



# 1. SONIC simulation for EU-DEMO divertor

**SOLPS mesh has been successfully converted from SOLPS-ITER to SONIC format.**

*Liner* is included in the private region and n-transport is performed to exhaust-slot.

**Poloidal mesh:** 26 below Xp, 47 along main plasma(JA-DEMO: 40 below Xp, 68 for main)

**Radial mesh:** 19 covers between  $r^{mid} = 0 - 7.6$  cm (JA-DEMO: 25  $r^{mid} = 0 - 3.2$ cm)

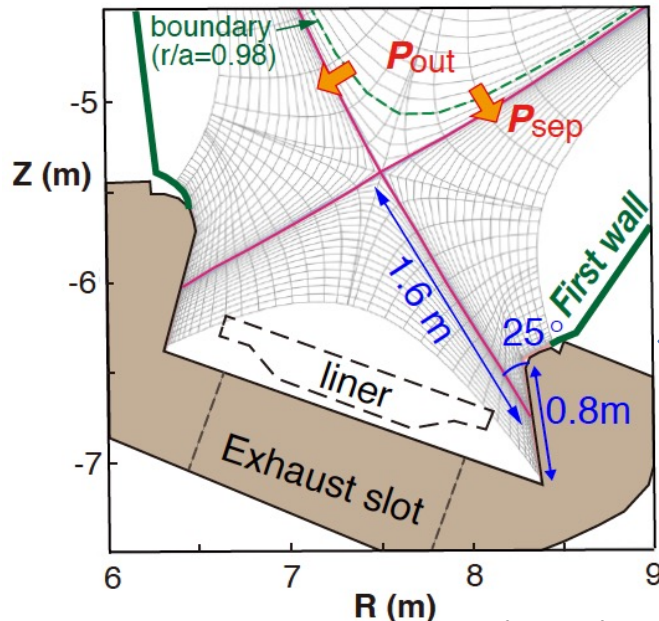
**Calculations with following parameters started from 2021/10 :**

Given at C-E boundary ( $r/a=0.98$ ):  $P_{out} = 160$  MW,  $\Gamma_{out} = 5 \times 10^{21}$

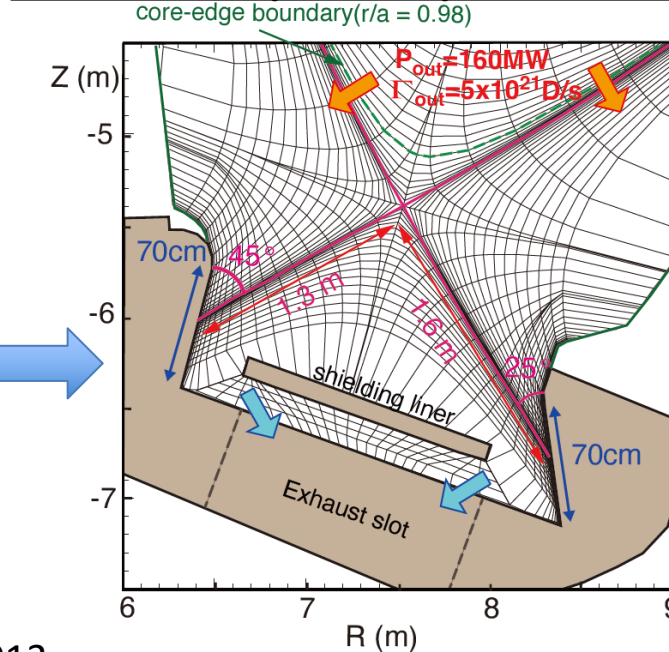
• **Total radiation loss ( $P_{rad}$ ) scan was performed by Ar seed feedback:**

3 cases:  $P_{rad} = 96, 112, 128$  MW ( $f_{rad} = P_{rad}/P_{out} = 0.6, 0.7, 0.8$ ).

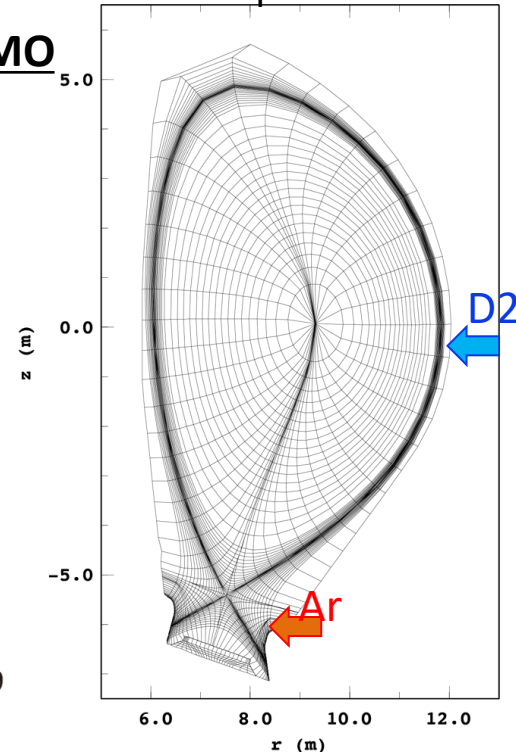
**SOLPS mesh for EU-DEMO (2019)**



**SONIC mesh (incl. MC) for EU-DEMO**



**Ar and D-puff locations**



**Exhaust parameters** are similar to those by SOLPS-ITER simulation (F.Subba NF2021):

- $P_{out} = 160$  MW,  $\Gamma_{out} = 5 \times 10^{21}$  D/s at C-E boundary : same as SOLPS.
- $\Gamma_{puff} = 4.8-9.6 \times 10^{22}$  D/s (similar to JA) was scanned: smaller than  $2 \times 10^{23}$  for SOLPS.
- $S_{pump} = 200$  m<sup>3</sup>/s : similar to SOLPS (R = 0.99022 corresponds to 200~210 m<sup>3</sup>/s)
- **Diffusion coefficients are a key parameter** (SONIC sets 1 area in Edge, 2 areas in SOL)
  - ⇒  $\chi$  was reduced to 0.2 m<sup>2</sup>/s both at Edge and SOL
  - ⇒ JA-DEMO cases ( $\chi=0.5$  or 1 m<sup>2</sup>/s,  $D=0.15$  or 0.3 m<sup>2</sup>/s) were also calculated.

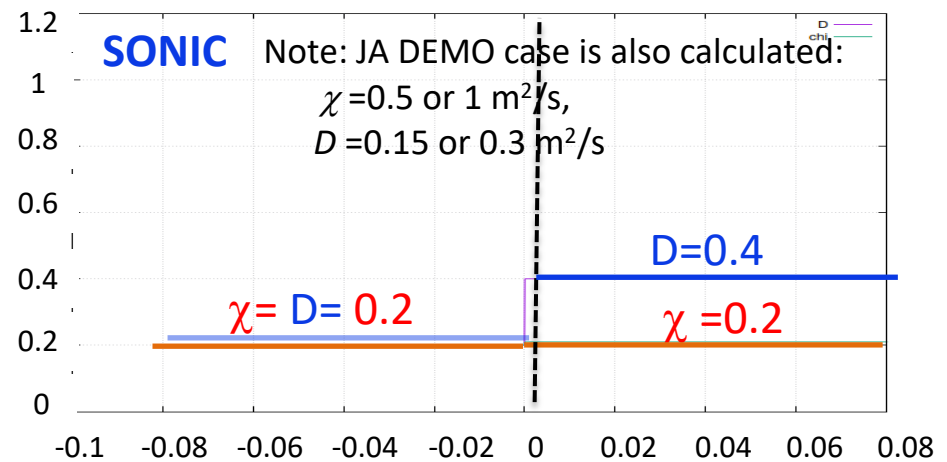
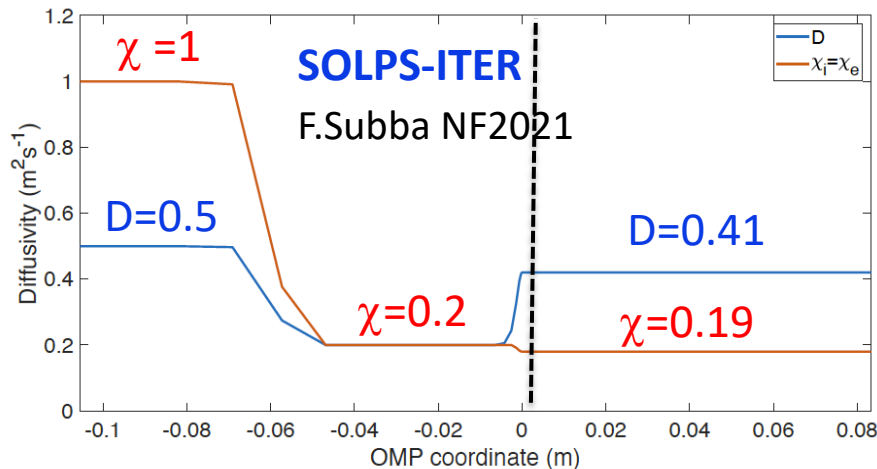


Figure 4. Transport coefficients used for the modeling described in this work.

For Ar impurity,  $D_{imp} = 0.3$  m<sup>2</sup>/s (in IMPMC)

- **Flux limiter (same)**: same as SOLPS

Ion heat flux:  $\alpha=10$     electron heat flux:  $\alpha=0.2$     viscosity:  $\alpha=0.5$



# Detachment is produced at outer-strike point ( $f_{rad}^{div} \sim 0.7$ )

Peak  $q_{target}$  is sensitive to D-puff rate ( $T_i, T_e$  profiles)

-6-

$D_2$ -puff rate is increased from  $4.8$  to  $7.2 \times 10^{22} D/s$  at the same Ar radiation fraction of  $f_{rad}^{div} = (P_{rad}^{sol} + P_{rad}^{div}) / P_{sep} \sim 0.7 \Rightarrow$  both  $n_e^{mid}$  and  $P_{rad}^{div-out}$  are increased.

- Narrow detachment ( $T_e^{div} < 2$  eV) is produced near the strike-point ( $r^{div} < 2$  cm).
- Peak  $q_{target}$  is seen at the boundary of attached plasma region ( $r^{div} \sim 2-3$  cm), which is significantly reduced from  $21$  to  $12.3$   $MWm^{-2}$  due to reduction of local  $T_e^{div}$  and  $T_i^{div}$ .

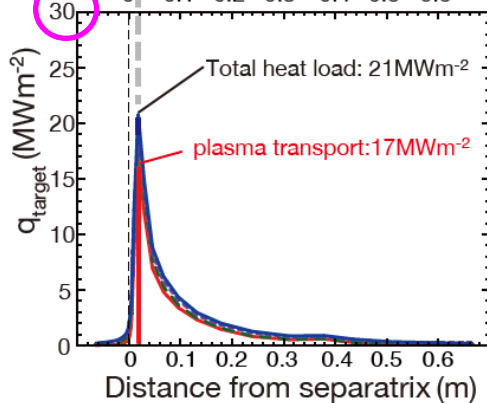
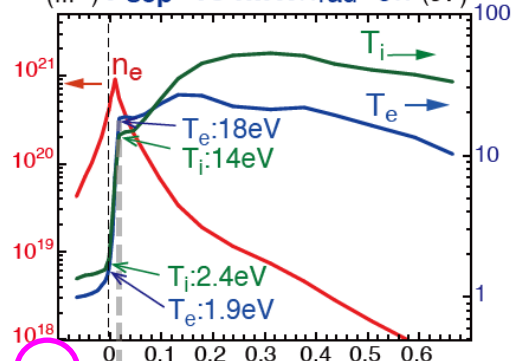
$n_e^{mid} \sim 2.1 \times 10^{19} m^{-3}$

$\Gamma_{puff}^{Ar} \sim 4.4 \times 10^{20} s^{-1}$

$P_{rad}^{div-o} \sim 24$  MW

$\Gamma_{puff} = 4.8 \times 10^{22} D/s$

$P_{sep} = 154$  MW /  $f_{rad} = 0.7$  (eV)



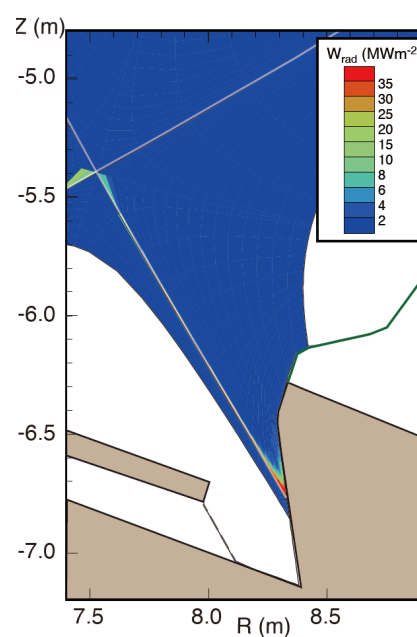
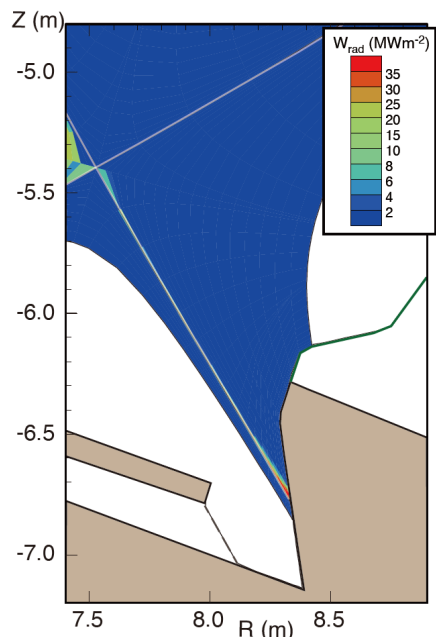
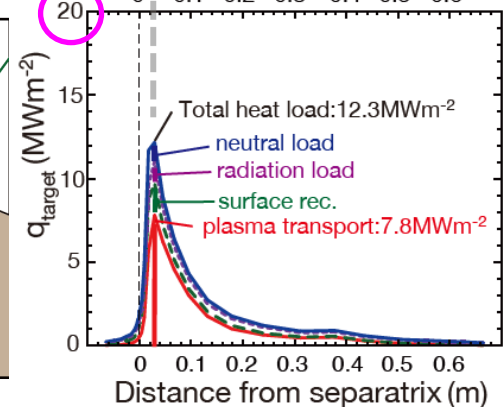
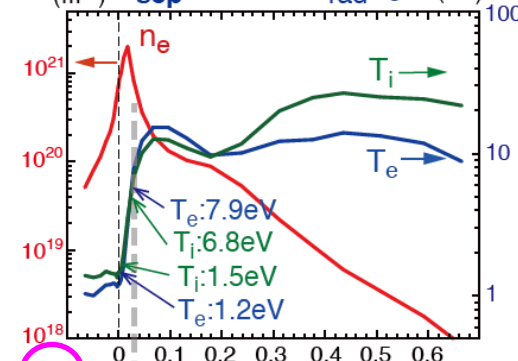
$n_e^{mid} \sim 2.4 \times 10^{19} m^{-3}$

$\Gamma_{puff}^{Ar} \sim 4.0 \times 10^{20} s^{-1}$

$P_{rad}^{div-o} \sim 34$  MW

$\Gamma_{puff} = 7.2 \times 10^{22} D/s$

$P_{sep} = 155$  MW /  $f_{rad} = 0.7$  (eV)



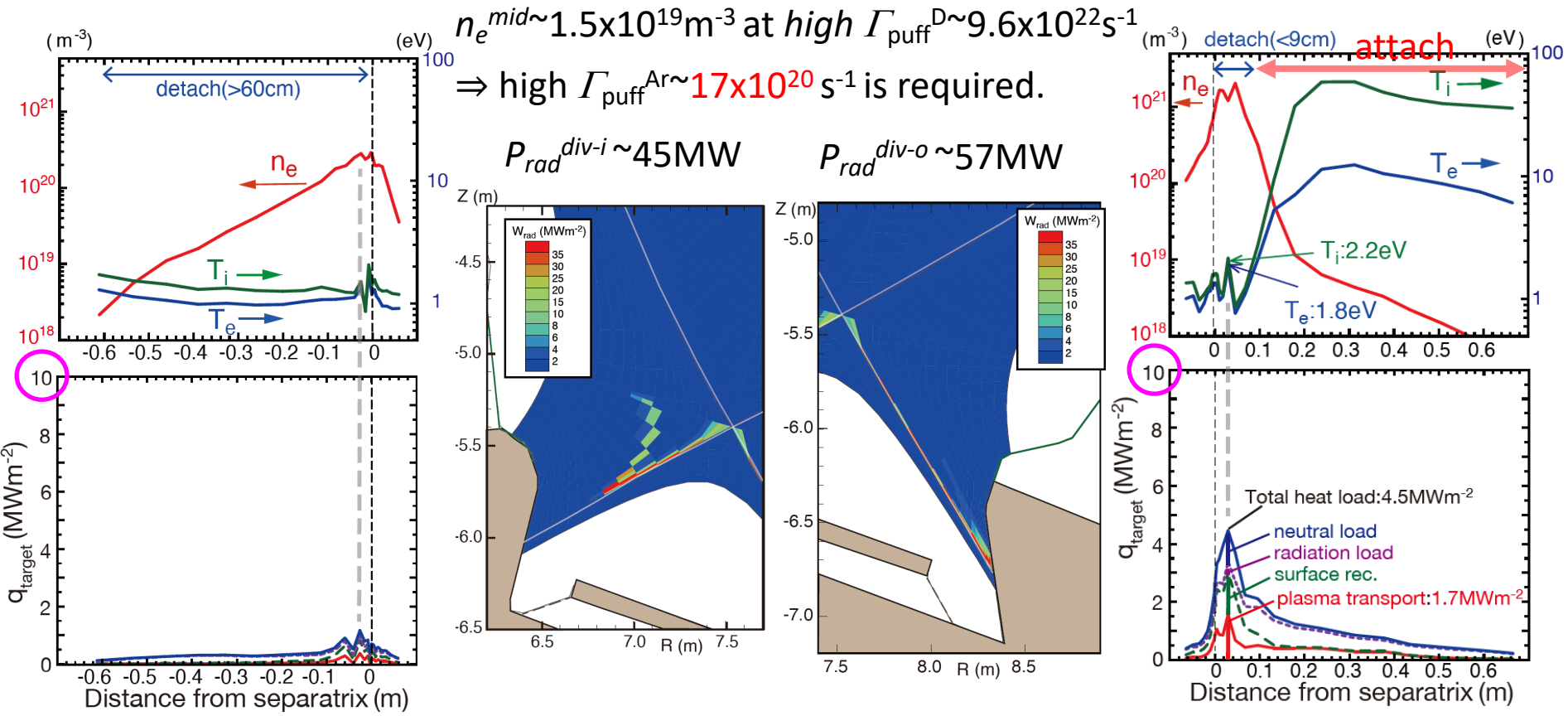


# Detachment is extended with increasing $P_{rad}$ ( $f_{rad}^{div} \sim 0.8$ )

Peak  $q_{target}$  is reduced below  $10 \text{ MWm}^{-2}$ , when detachment is extended.

Ar seeding is increased to  $f_{rad}^{div} \sim 0.8$  with Ar rate  $\sim 17 \times 10^{20} \text{ Ar/s}$  (4 times higher!) since SOL  $n_e^{mid}$  is reduced (from  $2.1 \times 10^{19}$ ) to  $1.5 \times 10^{19} \text{ m}^{-3}$ .

- Partial detachment is extended near the strike-point ( $r^{div} < 9 \text{ cm}$ ).
- Peak  $q_{target}$  appears in the detached region and is further reduced to  $4.5 \text{ MWm}^{-2}$ ; **plasma transport load is reduced**, and **surface rec. & neutral loadings** are increased.





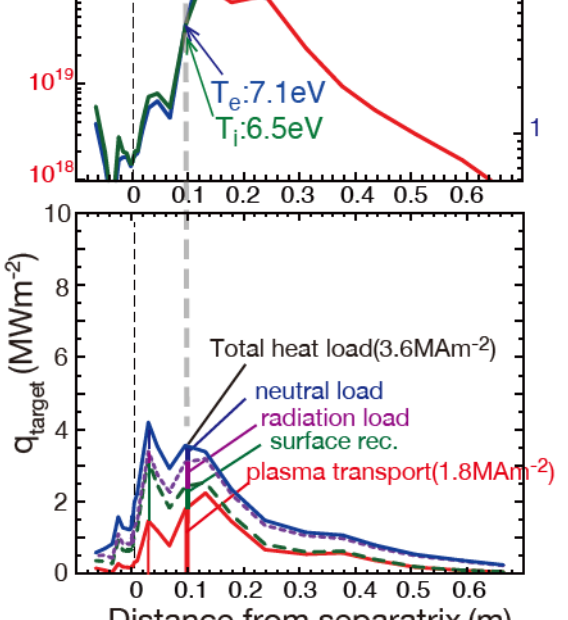
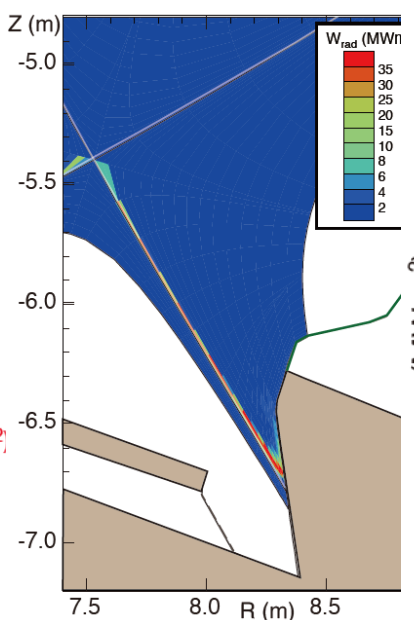
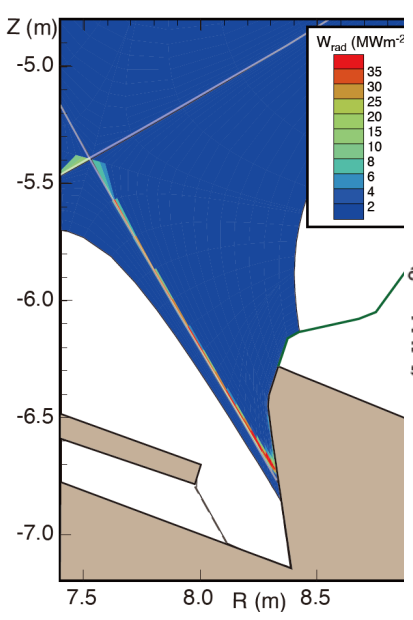
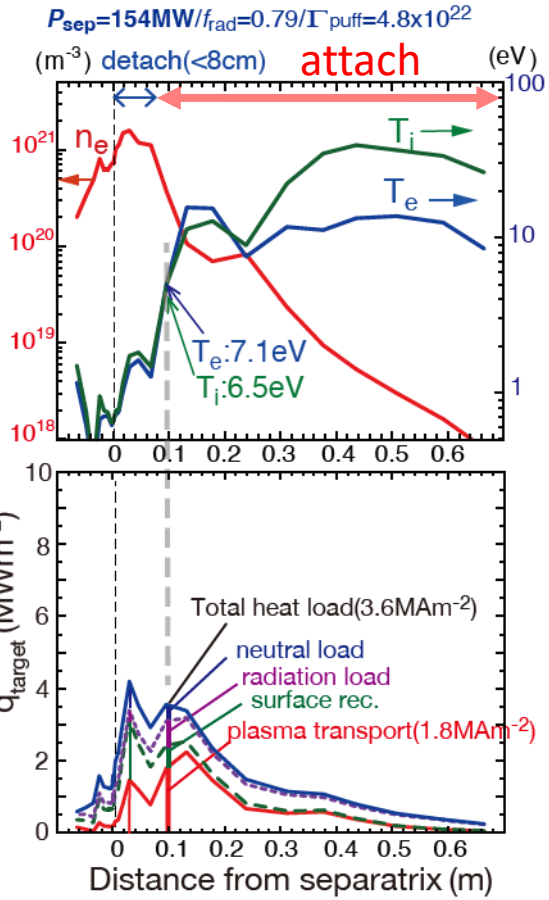
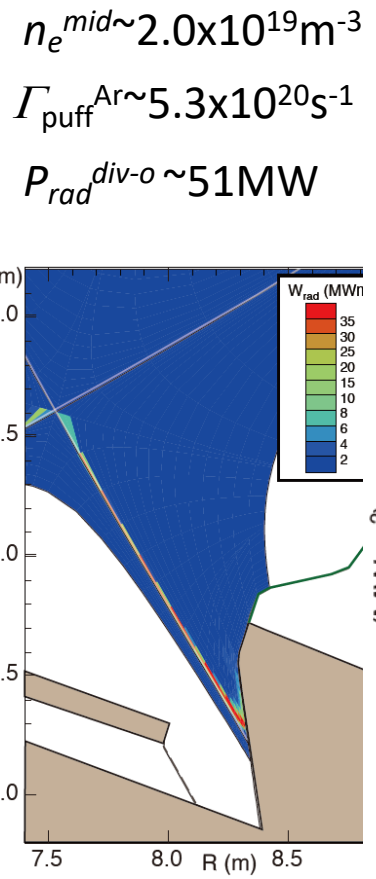
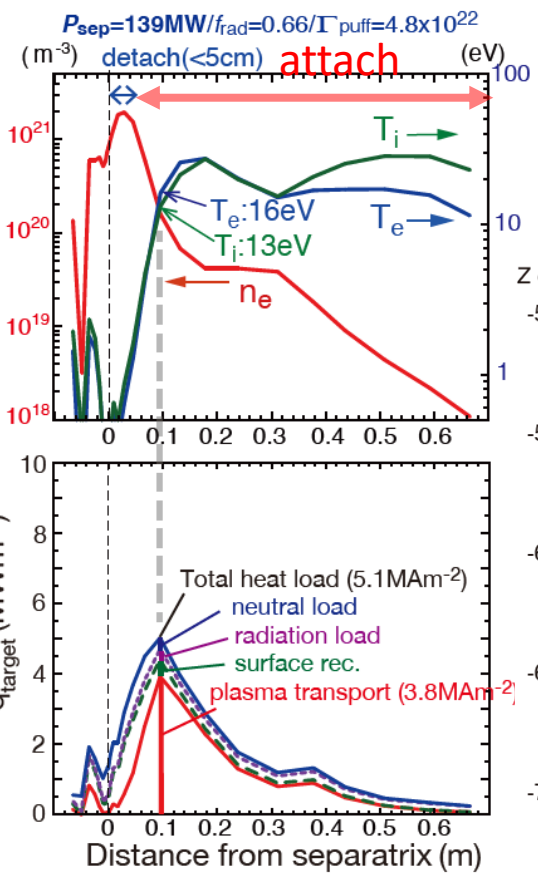
# $\chi, D$ for JA-DEMO simulation are applied ( $f_{\text{rad}}^{\text{div}}=0.7-0.8$ )

-8-

Diffusion coefficients for JA-DEMO (larger  $\chi$ :  $1.0\text{m}^2/\text{s}$ , smaller  $D$ :  $0.3$ ) are applied:  
Ar seeding is  $1.3 \times 10^{20}\text{Ar}/\text{s}$  ( $f_{\text{rad}}^{\text{div}} \sim 0.7$ ) and  $6.3 \times 10^{20}$  ( $f_{\text{rad}}^{\text{div}} \sim 0.8$ ): similar to JA DEMO.  
SOL  $n_e^{\text{mid}}$  is decreased from  $2.6 \times 10^{19}\text{m}^{-3}$  to  $2.0 \times 10^{19}\text{m}^{-3}$ .

- $f_{\text{rad}}^{\text{div}} \sim 0.7$ : Detachment is wider and peak  $q_{\text{target}}$  is reduced (in attached region).
- $f_{\text{rad}}^{\text{div}} \sim 0.8$ : Two  $q_{\text{target}}$  peaks appear in detached and attached regions; continuing cal.

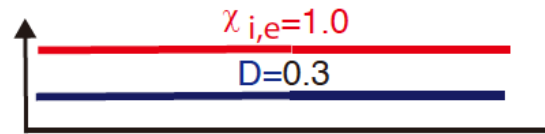
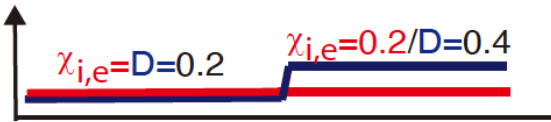
$n_e^{\text{mid}} \sim 2.6 \times 10^{19}\text{m}^{-3}$   
 $\Gamma_{\text{puff}}^{\text{Ar}} \sim 1.3 \times 10^{20}\text{s}^{-1}$   
 $P_{\text{rad}}^{\text{div-o}} \sim 35\text{MW}$





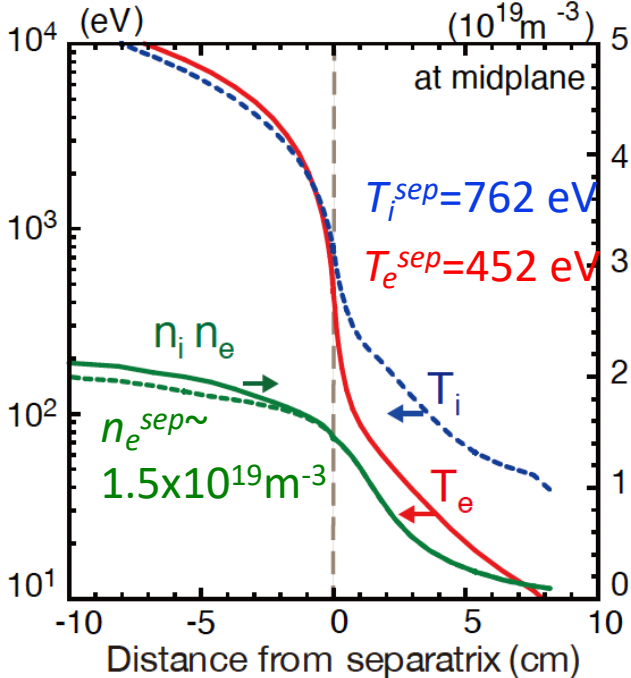
# Effect of diffusion coefficients on $T_e^{mid}$ and $T_i^{mid}$ profiles

- $T_e^{mid}$  and  $T_i^{mid}$  gradients are generally large for lower  $\chi$  cases ( $0.2\text{m}^2/\text{s}$ ):  $n_e^{sep}$  ( $1.5 \times 10^{19} \text{ m}^{-3}$ ) is lower, and  $T_e^{sep}$  (452 eV) and  $T_i^{sep}$  (762 eV) are higher.
- Fuel dilution is relatively small, whereas large Ar puff rate and low  $n_e^{mid}$   $\Rightarrow$  low radiation loss at edge and SOL regions.



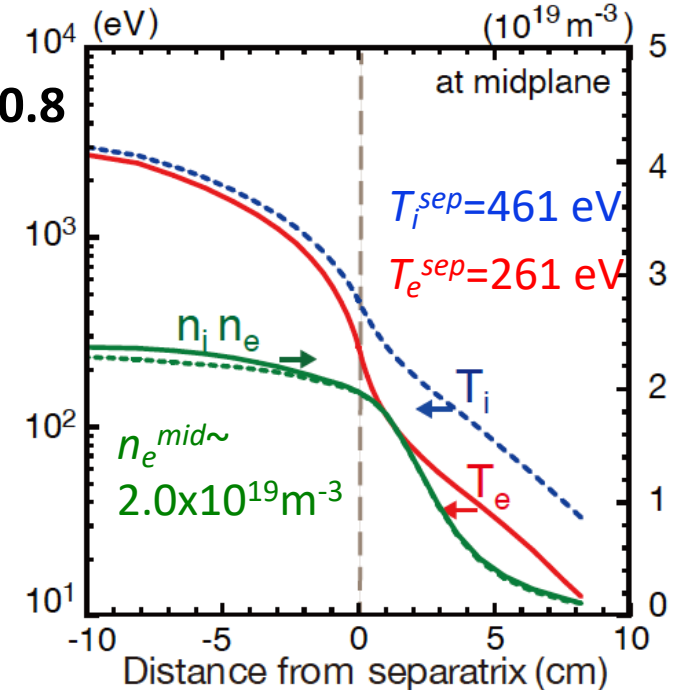
$\Gamma_{puff}^{Ar} \sim 17 \times 10^{20} \text{ s}^{-1}$

$P_{sep} = 152 \text{ MW} / f_{rad} = 0.8 / \Gamma_{puff} = 9.6 \times 10^{22}$



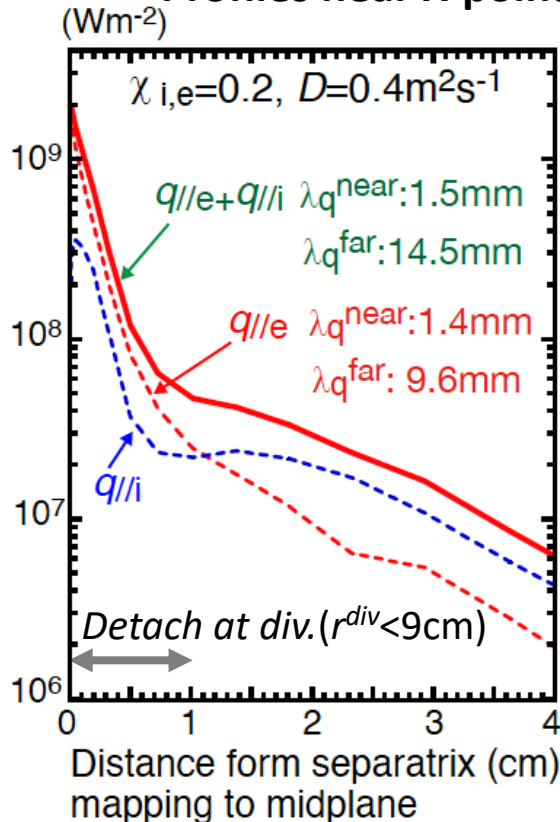
$\Gamma_{puff}^{Ar} \sim 5.3 \times 10^{20} \text{ s}^{-1}$

$P_{sep} = 154 \text{ MW} / f_{rad} = 0.79 / \Gamma_{puff} = 4.8 \times 10^{22}$



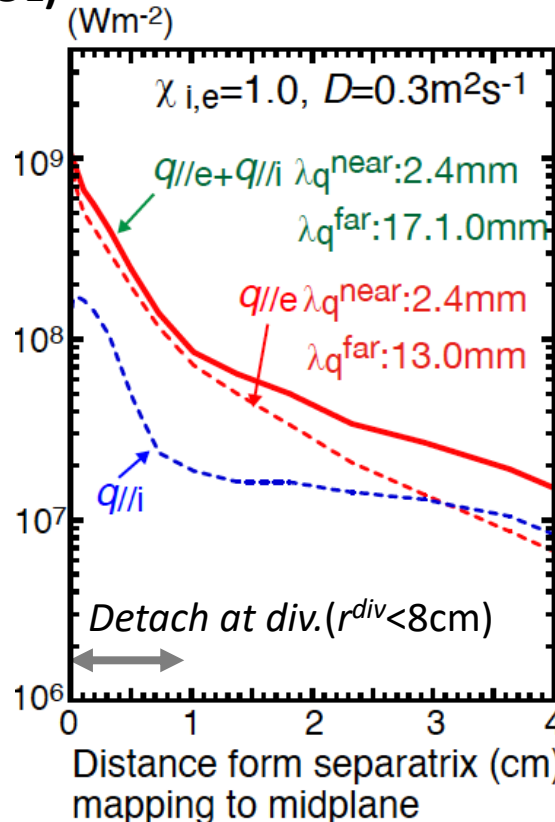
- Electron heat flux is dominant *near separatrix (near-SOL)*:  
decay length of *total heat flux* ( $\lambda_{q_i+q_e}^{near}$ ) is similar to that of *el. heat flux* ( $\lambda_{q_e}^{near}$ ).
- Ion heat flux becomes dominant *in the outer flux surfaces (far-SOL)*:  
⇒ “Shoulder” is produced in  $q_{i//}$  profile by ion (convective) transport.

## Profiles near X-point (LFS SOL)



$$1.44 \times 10^9 \exp(-r/\lambda_q^{near}) + 0.88 \times 10^8 \exp(-r/\lambda_q^{far})$$

$$1.95 \times 10^9 \exp(-r/\lambda_q^{near}) + 0.97 \times 10^8 \exp(-r/\lambda_q^{far})$$



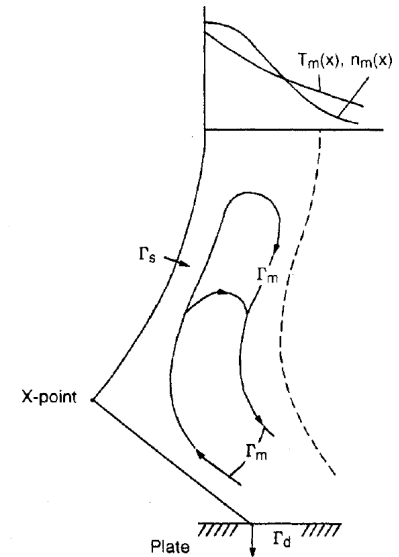
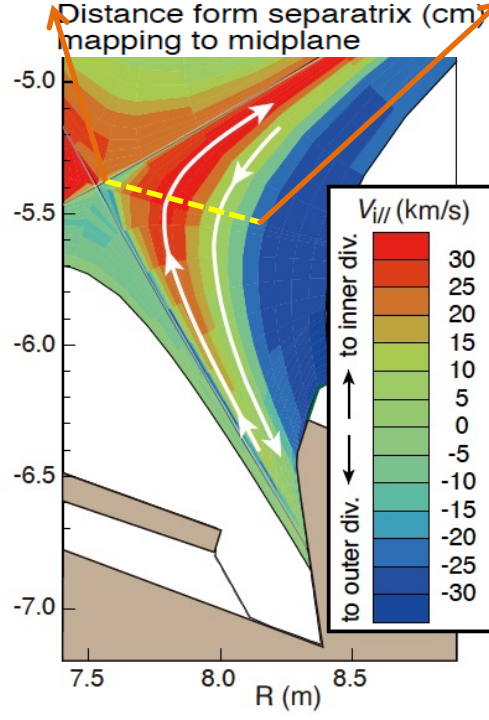
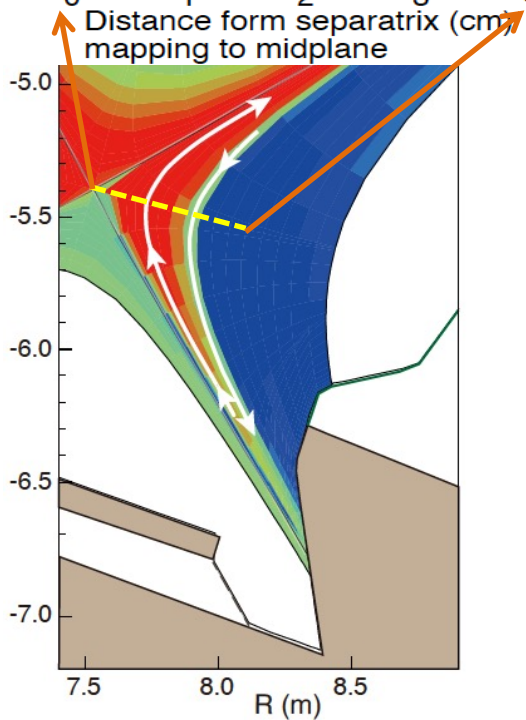
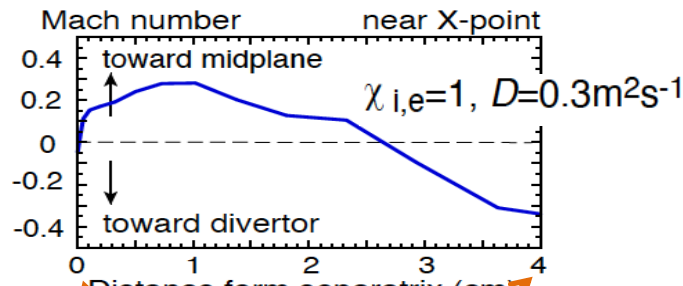
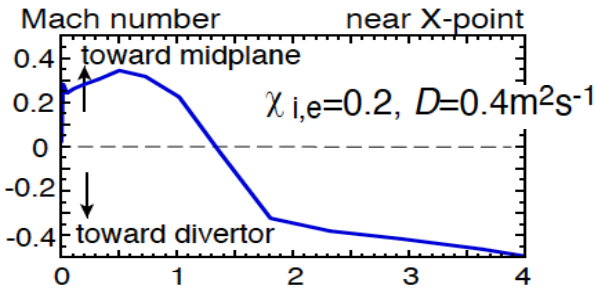
$$0.60 \times 10^9 \exp(-r/\lambda_q^{near}) + 0.80 \times 10^8 \exp(-r/\lambda_q^{far})$$

$$0.85 \times 10^9 \exp(-r/\lambda_q^{near}) + 1.94 \times 10^8 \exp(-r/\lambda_q^{far})$$

Noted that  $\lambda_{q_i+q_e}^{near} \sim 3.6\text{mm}$  (larger) for ITER simulation with the same  $\chi = 1$  &  $D = 0.3 \text{ m}^2\text{s}^{-1}$ .  
A.S.Kukushkin. et al., J. Nucl. Mater. 38 (2013) S203.

# “Flow reversal” ( $M_{//} = 0.2 \sim 0.4$ ) is produced above divertor target by locally increasing neutral ionization and plasma pressure

- *Ion convective transport produced by the flow reversal* contributes to ion heat flux towards the upstream SOL and produces a “shoulder” in the  $q_{//i}^{Xp}$  profile.
- *Flow reversal also reduced the impurity retention in the outer divertor*, which may sustain the attached plasma region and produce the partial detachment.



Ref. Krasheninnikov, et al.  
*Nucl. Fusion* 1992, 32, 1927.

On the other hand, the flow reversal from the outer target was NOT found in the major tokamak experiments, i.e., flow to the target (forward) direction was measured near the Xp.

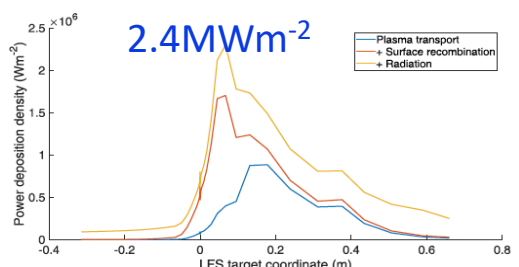
With support from EU experts, **SONIC simulations for EU DEMO divertor** have been carried out successfully with similar power exhaust parameters as EU SOLPS-ITER used.

- Radiation power scan ( $f_{\text{rad}} = P_{\text{rad}}/P_{\text{out}} = 0.6 \rightarrow 0.7 \rightarrow 0.8$ ) was performed for two diffusion coefficient cases ( $\chi = 0.2-0.3 \text{ m}^2\text{s}^{-1}$  used by EU SOLPS-ITER, and  $\chi = 1.0 \text{ m}^2\text{s}^{-1}$  used for JA DEMO).
  - Low  $\chi = 0.3 \text{ m}^2\text{s}^{-1}$  case, peak  $q_{\text{target}}$  was quickly reduced from  $26 \rightarrow 12 \sim 21 \rightarrow 4.5 \text{ MWm}^{-2}$ :  
**Peak  $q_{\text{target}}$  was seen at attach-detach boundary ( $r^{\text{div}} \sim 3\text{cm}$ ), which is sensitive to  $T_e^{\text{div}}, T_i^{\text{div}}$  profiles.**  
**For  $f_{\text{rad}} = 0.8$ , peak  $q_{\text{target}}$  appeared at detached region: plasma load was significantly reduced.**
  - High  $\chi = 1 \text{ m}^2\text{s}^{-1}$  case, peak  $q_{\text{target}}$  was gradually reduced from  $12 \rightarrow 5.5 \rightarrow 3.5 \sim 4 \text{ MWm}^{-2}$ :  
**Peak  $q_{\text{target}}$  became comparative when it appeared at the detached region.**
  - Effects of diffusion and ion transport (flow reversal) on  $q_{\parallel}$ -profile and divertor were investigated.
- ⇒ Distributions of upstream SOL plasma ( $q_{i,e/\parallel}, \chi_{\parallel}$  and plasma flow) and impurity (thermal and friction forces) will be compared for comparable input condition on SONIC & SOLPS-ITER.

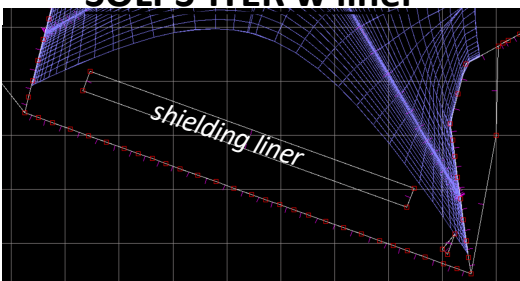
**EU SOLPS-ITER simulations are now on-going with 2 focusses:**

- Effect of **shielding liner** of the DEMO divertor,
- Simulation in *new equilibrium variant released in 2021 with higher B-field*, which will affect the divertor detachment.

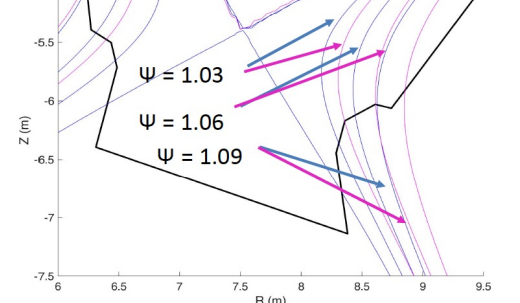
**SOLPS-ITER result: w/o Liner ( $f_{\text{rad}} \sim 0.8$ )**



**SOLPS-ITER w liner**



**new equilibrium (larger expansion)**







# He concentration in detached divertor

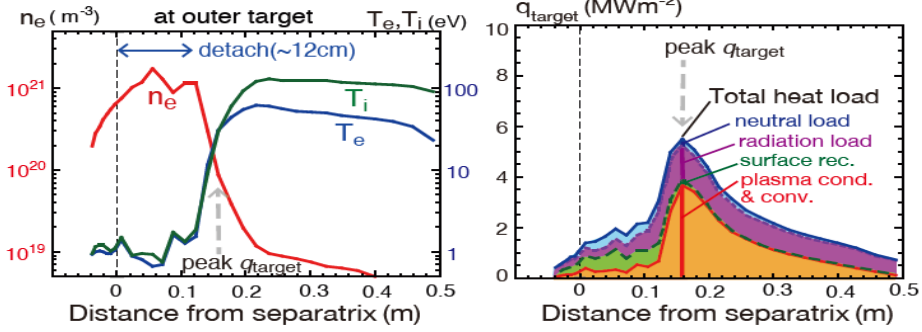
$C_{He}^{edge} = 4-7\%$  similar to exhausting  $\Gamma_{He}/\Gamma_D$ : Accumulation of He is NOT seen.

With increasing gas puff rate, *detachment width* increases and *peak  $q_{target}$*  is reduced.

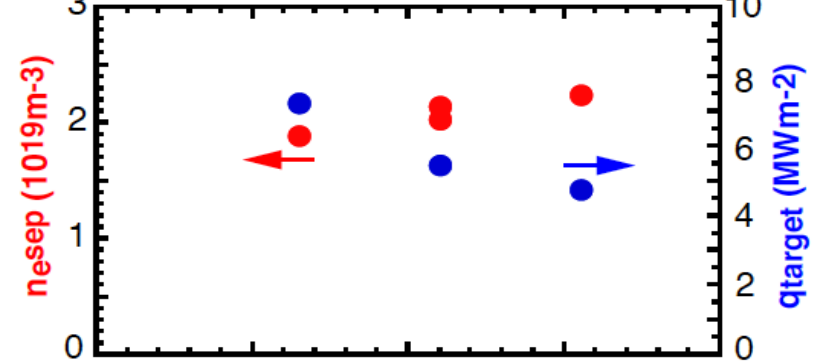
He concentrations at SOL and plasma edge ( $C_{He}^{edge} = n_{He}^{edge}/n_D^{edge}$ ):

- In-out asymmetry of  $C_{He}$  in SOL/divertor is 2-3 times, but decreasing near separatrix.
- $C_{He}^{edge} = 4-7\%$  at plasma edge (smaller than SOL)  $\Rightarrow$  Accumulation of He is NOT seen.

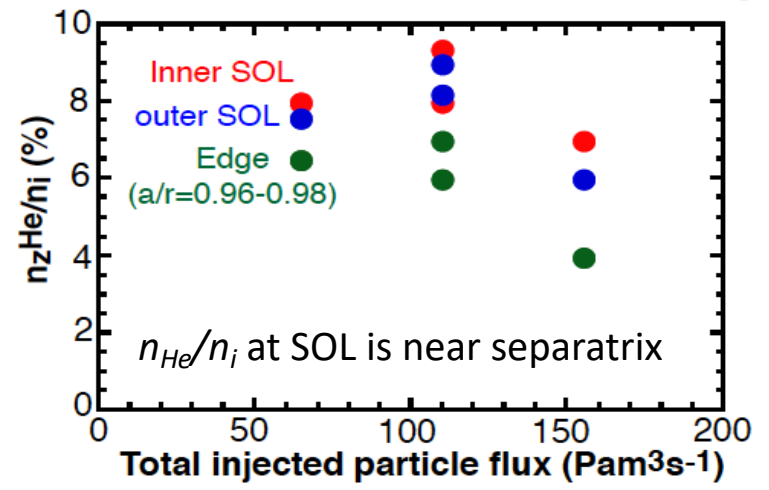
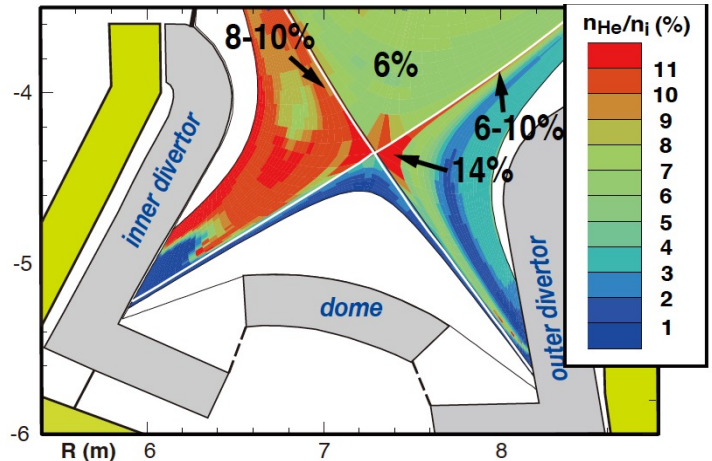
## Profiles of plasma and heat load at outer target:



## Midplane density and peak heat load



## He concentration ( $n_{He}/n_i$ ) in divertor



He concentration result in the detached divertor for **EU DEMO using SOLPS-ITER**:

- $C_{He}^{edge} = n_{He}^{edge} / n_D^{edge} \sim 20\%$  was beyond acceptable limit of fuel dilution.

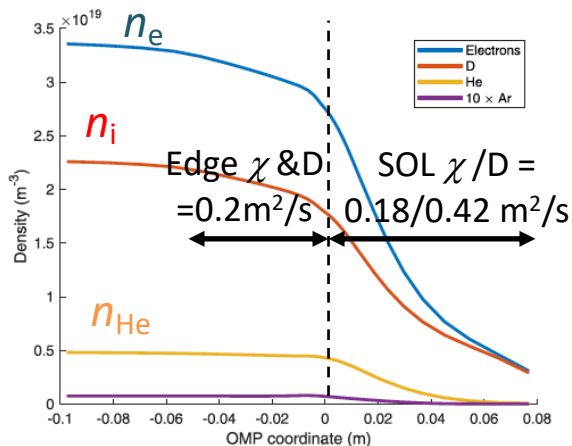
## SONIC simulation for JA DEMO divertor:

Diffusion coefficients were reduced to half values ( $\chi:0.5, D:0.15 \text{ m}^2\text{s}^{-1}$ ).

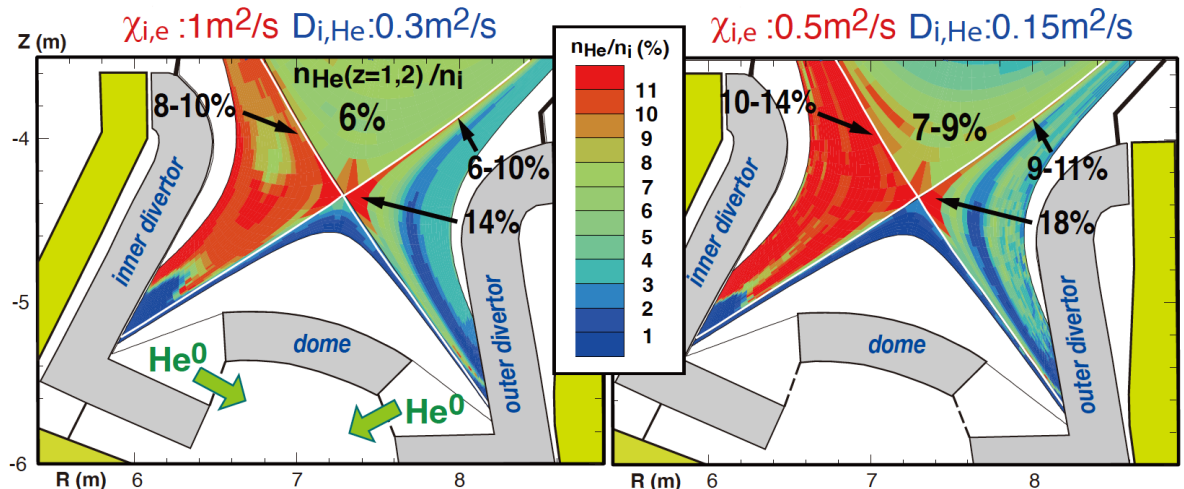
- *Detachment width* decreased and *peak  $q_{target}$*  was increased from 5.5 to 7.8  $\text{MWm}^{-2}$ .
- $C_{He}$  at inner, outer SOLs and Xp were enhanced to 10-14%, 9-11% and 18%, respectively.
- $C_{He}^{edge}$  is increased from 4-7% to 7-9%, which is larger than  $\Gamma_{He} / \Gamma_D \sim 5\%$ , but **still acceptable level** (below the design value:  $n_{He} / n_e \sim 7\%$ ).

## He profile in EU DEMO edge

$n_{He} / n_i \sim 20\%, n_{He} / n_e \sim 14\%$



## He concentration ( $n_{He} / n_i$ ) in JA DEMO divertor





# Progress summary: He exhaust simulations for JA-DEMO

-16-

- Larger exhaust power ( $P_{sep} \sim 250$  MW), lower SOL density ( $n_e^{sep} = 2-3 \times 10^{19} \text{m}^{-3}$ ) than ITER.  
⇒ He ion flux equivalent to  $P_{fusion} = 1.5$  GW was exhausted from edge ( $r/a \sim 0.95$ ), and He densities in the divertor and edge were evaluated with enhancing the detachment.
- With increasing detachment width by increasing gas puff rate (but same  $f_{rad}^{div} \sim 0.8$ ), accumulation of He ion was not seen in the plasma edge:  $(n_{He}/n_D)^{edge} \sim 4-7\%$ .
- Reduction of diffusion coefficients to half values increased  $(n_{He}/n_D)^{edge}$  to 7-9%, which is still acceptable, but further increase should be avoided.  
⇒ Further reduction of edge  $\chi$  to 0.2-0.3  $\text{m}^2\text{s}^{-1}$  ( $D = 0.2$  is similar now) is planned.  
⇒ Divertor geometry effect (such as dome size) and requirements of pumping speed/divertor pressure will be evaluated.

Recent progresses of modelling to evaluate influences under the DEMO condition:

- **Kinetic models (thermal force on impurity transport and flux limiter for ion conduction)** for low collisionality SOL in DEMO were developed
- **Elastic collision model** of D-D, D-D2, D2-D2, D-He was incorporated, and during improvement.

## Future activities :

- **Benchmark of SONIC and SOLPS-ITER codes** both for EU- and JA-DEMOS (BA DDA).
- **Integration of transport codes, SONIC and TOPICS (main plasma)**, is in progress.
- **Renewing SOLDOR to incorporate drifts** is considered.

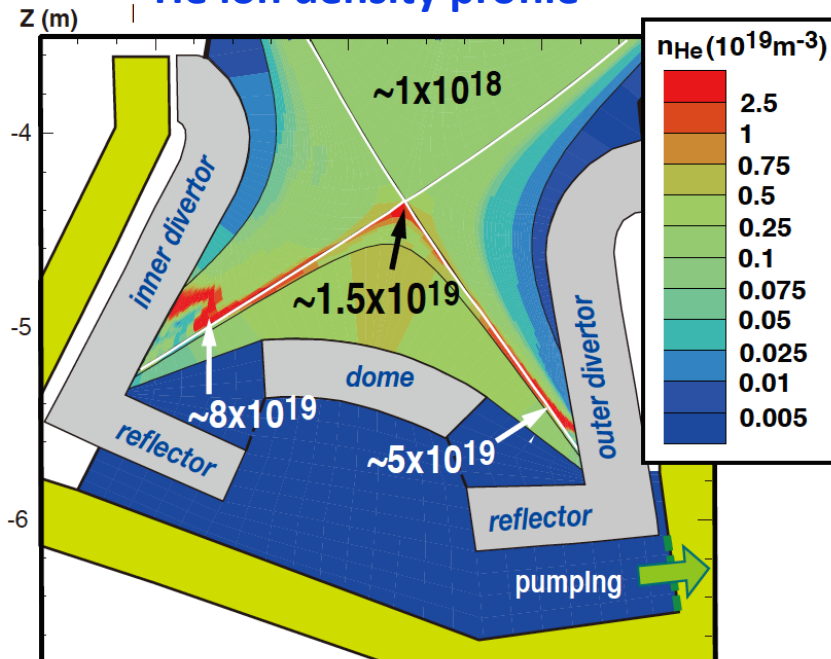


# Profiles of He ion density in divertor and plasma edge

## He ion density in divertor and plasma edge :

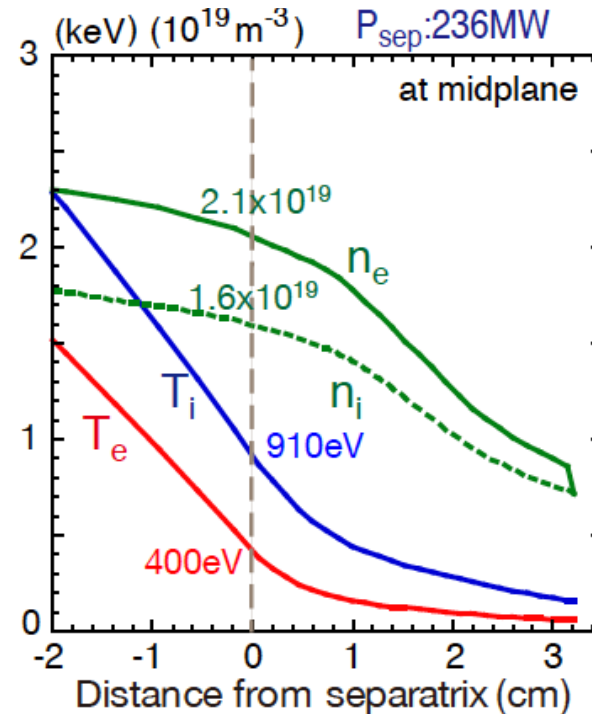
- He ion density ( $n_{He}$ ) is significantly increased near the detachment front (between Ar radiation peak and D ionization front) due to recycling in the divertor.
- $n_{He}$  is increased also near X-point (similar to  $D^+$  density).
- $n_{He} \sim 1 \times 10^{18} \text{ m}^{-3}$  inside the separatrix ( $r^{mid}/a = 0.96-0.98$ ):  
 $n_e^{mid}$  is 25% larger than  $n_i^{mid}$  due to Ar and He ions (similar contributions to  $\Delta n_e^{mid}$ ).

## He ion density profile



Elastic collision of  $He^+-D^+$ ,  $He^{++}-D^+$  are not included

## Plasma profiles at outer midplane





# Plasma detachment and $D^0/D_2$ pressure in divertor

Wider reflector angle: plasma detachment and neutral pressure were similar

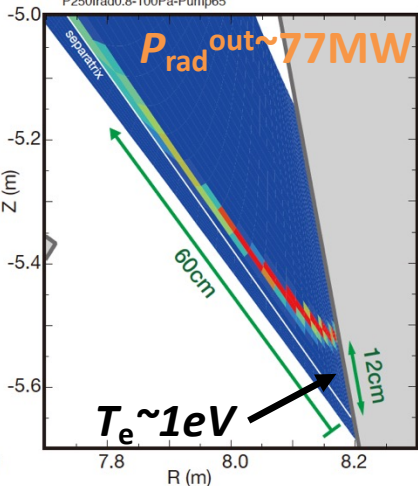
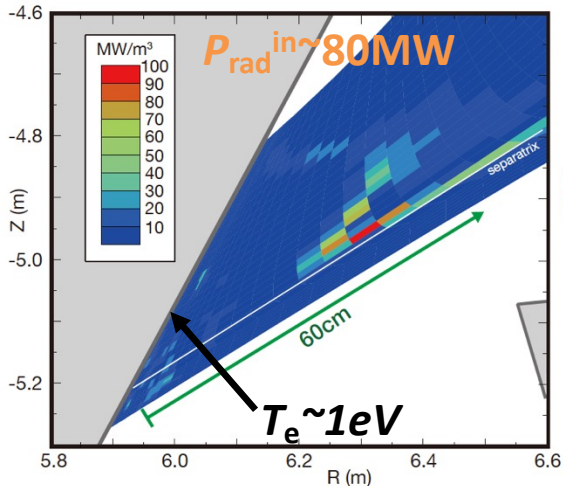
Gas puff  $5.3 \times 10^{22} D/s$  and Ar seeding:  $3.9 \times 10^{20} Ar/s$ ,

$$f_{rad}^{*div} = (P_{rad}^{sol} + P_{rad}^{div}) / P_{sep} = 0.78 \quad (0.04 \text{ for He radiation})$$

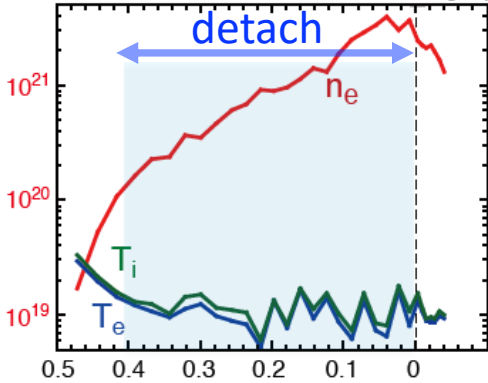
Inner target: Full detachment ( $T_{e,i} \sim 1eV$ )

Outer target: Partial detachment ( $T_{e,i} \sim 1eV$  in  $r^{div} < 12 \text{ cm}$ )

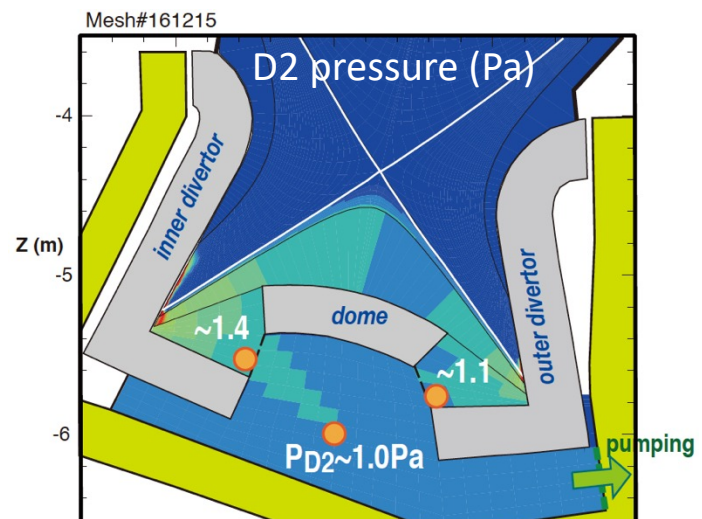
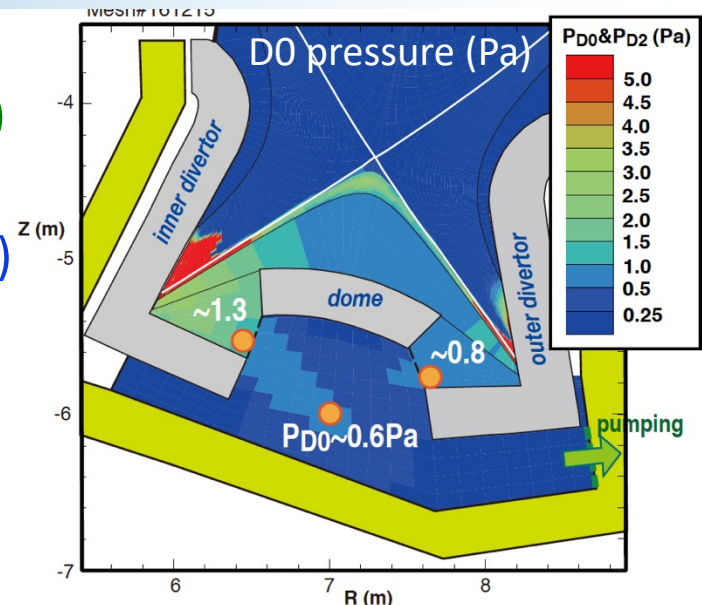
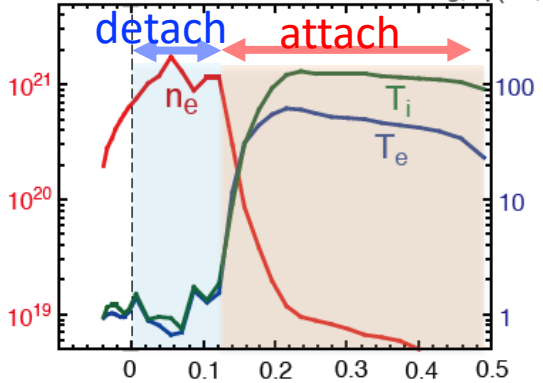
$P_{D2}$  and  $P_{D0}$  are comparable at exhaust slots.



$n_e$  ( $m^{-3}$ ) at inner target



$n_e$  ( $m^{-3}$ ) at outer target



Elastic collisions of  $D0-D0$ ,  $D0-D2$ ,  $D2-D2$  etc. are not considered.

# Distribution of He atom density in detachment

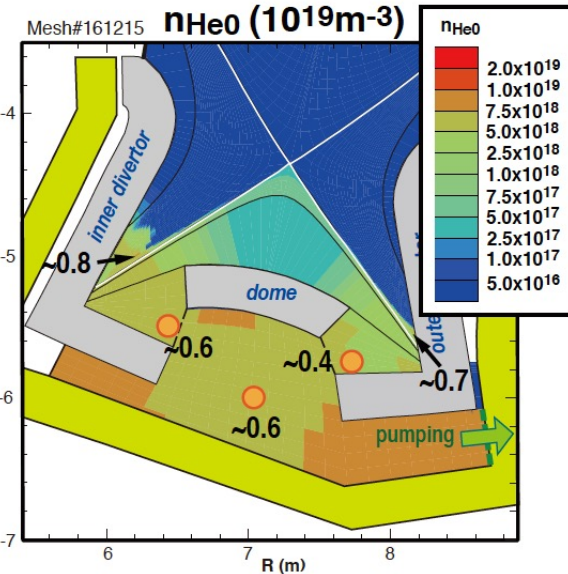
$n_{He0}/n_{D2}$  in the divertor is also 4-6%, similar to that at the plasma edge

- Neutral pressure ( $P_{D2}+P_{D0}$ ) in the divertor is increased with gas puff rate.
- Note: for large throughput cases, exhaust flux is smaller than total injected D flux.

## He atom density ( $n_{He}$ ) in the divertor :

- $n_{He0}$  increases downstream of the ionization front.
- $n_{He0}$  and  $n_{D2}$  are relatively uniform in the divertor
- $\Rightarrow n_{He0}/n_{D2}$  is 4-6%: similar to that at the plasma edge.

### He atom density profile



### D gas density profile

